


## RESEARCH ARTICLE

# A discriminative event-based model for subtype diagnosis of sporadic Creutzfeldt-Jakob disease using brain MRI

Vikram Venkatraghavan<sup>1,2,3</sup> | Riccardo Pascuzzo<sup>4</sup>  | Esther E. Bron<sup>1</sup> |  
Marco Moscatelli<sup>4</sup> | Marina Grisoli<sup>4</sup> | Amy Pickens<sup>5</sup> | Mark L. Cohen<sup>5,6,7</sup> |  
Lawrence B. Schonberger<sup>8</sup> | Pierluigi Gambetti<sup>6</sup> | Brian S. Appleby<sup>5,6,7,9</sup> |  
Stefan Klein<sup>1</sup> | Alberto Bizzi<sup>4</sup>

<sup>1</sup>Biomedical Imaging Group Rotterdam, Department of Radiology & Nuclear Medicine, Erasmus MC, University Medical Center Rotterdam, Rotterdam, the Netherlands

<sup>2</sup>Alzheimer Center Amsterdam, Neurology, Vrije Universiteit, Amsterdam UMC, location VUmc, Amsterdam, the Netherlands

<sup>3</sup>Amsterdam Neuroscience, Neurodegeneration, Amsterdam, the Netherlands

<sup>4</sup>Neuroradiology Unit, Fondazione IRCCS Istituto Neurologico Carlo Besta, Milan, Italy

<sup>5</sup>National Prion Disease Pathology Surveillance Center, Case Western Reserve University, School of Medicine, Cleveland, Ohio, USA

<sup>6</sup>Department of Pathology, Case Western Reserve University, School of Medicine, Cleveland, Ohio, USA

<sup>7</sup>Department of Neurology, Case Western Reserve University, University Hospitals Cleveland Medical Center, Cleveland, Ohio, USA

<sup>8</sup>National Center for Emerging and Zoonotic Infectious Diseases, Centers for Disease Control and Prevention, Atlanta, Georgia, USA

<sup>9</sup>Department of Psychiatry, Case Western Reserve University, University Hospitals Cleveland Medical Center, Cleveland, Ohio, USA

## Correspondence

Riccardo Pascuzzo, Neuroradiology Unit,  
Fondazione IRCCS Istituto Neurologico Carlo  
Besta, Via Celoria 11, 20133 Milan, Italy.  
Email: [riccardo.pascuzzo@istituto-besta.it](mailto:riccardo.pascuzzo@istituto-besta.it)

Vikram Venkatraghavan and Riccardo  
Pascuzzo share first authorship.

## Funding information

European Union's Horizon 2020 research and  
innovation programme, Grant/Award Number:  
666992; CDC, Grant/Award Number:  
NU2GCK000434; Italian Ministry of Health;  
CJD Foundation

## Abstract

**Introduction:** Sporadic Creutzfeldt-Jakob disease (sCJD) comprises multiple subtypes (MM1, MM2, MV1, MV2C, MV2K, VV1, and VV2) with distinct disease durations and spatiotemporal cascades of brain lesions. Our goal was to establish the *ante mortem* diagnosis of sCJD subtype, based on patient-specific estimates of the spatiotemporal cascade of lesions detected by diffusion-weighted magnetic resonance imaging (DWI).

**Methods:** We included 488 patients with autopsy-confirmed diagnosis of sCJD subtype and 50 patients with exclusion of prion disease. We applied a discriminative event-based model (DEBM) to infer the spatiotemporal cascades of lesions, derived from the DWI scores of 12 brain regions assigned by three neuroradiologists. Based on the DEBM cascades and the prion protein genotype at codon 129, we developed and validated a novel algorithm for the diagnosis of the sCJD subtype.

**Results:** Cascades of MM1, MM2, MV1, MV2C, and VV1 originated in the parietal cortex and, following subtype-specific orderings of propagation, went toward the striatum, thalamus, and cerebellum; conversely, VV2 and MV2K cascades showed a striatum-to-cortex propagation. The proposed algorithm achieved 76.5% balanced

This is an open access article under the terms of the [Creative Commons Attribution-NonCommercial-NoDerivs](https://creativecommons.org/licenses/by-nc-nd/4.0/) License, which permits use and distribution in any medium, provided the original work is properly cited, the use is non-commercial and no modifications or adaptations are made.

© 2023 The Authors. *Alzheimer's & Dementia* published by Wiley Periodicals LLC on behalf of Alzheimer's Association.

accuracy for the sCJD subtype diagnosis, with low rater dependency (differences in accuracy of  $\pm 1\%$  among neuroradiologists).

**Discussion:** *Ante mortem* diagnosis of sCJD subtype is feasible with this novel data-driven approach, and it may be valuable for patient prognostication, stratification in targeted clinical trials, and future therapeutics.

#### KEYWORDS

Creutzfeldt-Jakob disease, diffusion-weighted MRI, discriminative event-based modeling, disease progression, prion disease, subtype diagnosis

#### Highlights

- Subtype diagnosis of sporadic Creutzfeldt-Jakob disease (sCJD) is achievable with diffusion MRI.
- Cascades of diffusion MRI abnormalities in the brain are subtype-specific in sCJD.
- We proposed a diagnostic algorithm based on cascades of diffusion MRI abnormalities and demonstrated that it is accurate.
- Our method may aid early diagnosis, prognosis, stratification in clinical trials, and future therapeutics.
- The present approach is applicable to other neurodegenerative diseases, enhancing the differential diagnoses.

## 1 | BACKGROUND

Sporadic Creutzfeldt-Jakob disease (sCJD), the most common form of human prion disease, is a rare and fatal neurodegenerative condition caused by the misfolding of the normal or cellular prion protein (PrP<sup>C</sup>) into a pathogenic or disease-related isoform (PrP<sup>D</sup>), which self-replicates, propagates, and typically accumulates in the brain.<sup>1–3</sup> Seven distinct and “pure” sCJD subtypes (MM1, MM2, MV1, MV2C, MV2K, VV1, and VV2) have been identified to date, mostly determined by the pairing of two factors: the polymorphism (methionine (M) or valine (V)) at codon 129 of the PrP<sup>C</sup> gene (*PRNP129*) and the type 1 or 2 of the proteinase K-resistant PrP<sup>D</sup>.<sup>4–9</sup> The sCJD subtypes substantially differ for disease duration and other clinical characteristics: patients with MM1 and MV1 subtypes present with cognitive decline and myoclonus, and show a fast progression (median: 3 to 4 months); VV2 and MV2K present with initial cerebellar symptoms and longer disease duration (median: 6.5 and 17 months, respectively), whereas MM2 and MV2C show striking cognitive deficits and longer durations (median: 16 months).<sup>8,10</sup>

Currently, the definite diagnosis of sCJD and its subtyping are established only *post mortem* by brain tissue examination. *Ante mortem* identification of the sCJD subtype would be important for the prognosis and the clinical management of these patients. Moreover, the possibility of discriminating subtypes can be helpful in the design of clinical trials. Current evidence indicates *PRNP129* genotype is an important factor in the evaluation of therapeutic treatments<sup>11</sup>, and

that any candidate therapeutic strategy for prion disease should be tested against multiple prion strains or subtypes.<sup>12</sup>

Magnetic resonance imaging (MRI) is one of the two most accurate tests for the *ante mortem* diagnosis of sCJD when diffusion-weighted imaging (DWI) is utilized.<sup>13–18</sup> A recent study has strengthened the role of MRI in sCJD diagnosis by demonstrating that DWI abnormalities appear focally, in one brain region, and propagate to other regions following a subtype-specific spatiotemporal cascade.<sup>19</sup> That study applied an event-based model (EBM)<sup>20,21</sup> to analyze the ratings assigned by neuroradiologists to diffusion MRI collected from a large cohort of patients affected by autopsy-confirmed sCJD. Based on the same dataset, another recent study showed that DWI can also provide an accurate *ante mortem* diagnosis of sCJD subtype, using decision tree algorithms.<sup>22</sup>

The present work aims to diagnose *ante mortem* the sCJD subtype with diffusion MRI by introducing a novel diagnostic algorithm that was inspired by the study<sup>19</sup> of the spatiotemporal cascades but it followed a different approach from the previously used decision trees<sup>22</sup> to address subtype diagnosis. Here, we relied on a discriminative event-based model (DEBM), a novel data-driven disease progression model,<sup>23,24</sup> to estimate the subtype-specific spatiotemporal cascades of DWI abnormalities from neuroradiologist ratings. The DEBM's main novelty is the computation of a single-time-point-based approximation of the spatiotemporal cascade observed in the examined patient which, following the comparative analysis with each subtype-specific cascade, leads to the identification of the most probable sCJD subtype.

## 2 | METHODS

### 2.1 | Patients

Patients were selected from a previously published<sup>13,19,22</sup> large cohort of subjects with suspected prion disease, recruited from January 2003 to April 2020 by the National Prion Disease Pathology Surveillance Center (Cleveland, Ohio, USA), as part of an MRI consultation service program. For this study, we included patients matching the following criteria: (i) diagnosis of pure subtype sCJD at autopsy and (ii) at least one positive brain DWI examination according to the evaluation of one neuroradiologist (A.B.). Moreover, 50 subjects with clinically suspected prion disease that was ruled out by autopsy, were randomly selected from the same published cohort<sup>13</sup> and used as negative controls for an inter-rater analysis that involved also other two neuroradiologists. This research project was approved by the University Hospitals Cleveland Medical Center institutional review board and by the local ethics committee of Fondazione IRCCS Istituto Neurologico Carlo Besta. Informed consent was waived on all the subjects, who were anonymized decedents.

### 2.2 | Biomarker collection and processing

The diagnosis of prion disease was established by brain histopathological examination, including prion protein immunohistochemistry and Western blot analysis.<sup>2,7</sup> Pure subtype of sCJD was defined by the detection of only one type (1 or 2) of PrP<sup>D</sup> from the Western blot examination of three brain regions and by the presence of only one neuropathological phenotype based on the histological examination of 17 brain regions. The phenotype was then required to match that associated with the pairing of the *PRNP129* genotype (MM, MV, or VV) with the PrP<sup>D</sup> type.

A senior neuroradiologist (A.B., 17 years of experience) had prospectively scored all diffusion MRIs in electronic format, blind to the clinical data and preliminary diagnosis, evaluating the presence of DWI signal hyperintensities in 12 brain regions on a four-point ordinal scale, as previously described.<sup>13</sup> Briefly, DWI signal hyperintensities were scored from zero (minimum, corresponding to the absence of any sCJD-related lesion) to three (maximum, presence of extensive sCJD-related lesions). Five neocortical regions (frontal, parietal, including the precuneus, temporal, and occipital lobes), three limbic structures (cingulate, insula, and hippocampus), striatum (caudate and putamen), thalamus, and cerebellum were evaluated. MRI examination was considered positive if at least one of these 12 regions was scored 2 or 3.

To assess rater-dependency, two other neuroradiologists, a senior (M.G.) with 17 years of experience and a junior (M.M.) with 2 years of experience, were asked to attribute negative (i.e., 0 and 1) and positive scores (i.e., 2 and 3) using the same scoring system described above. After a short training session on cases not included in the subsequent analysis, they scored a subgroup of 150 randomly selected

### RESEARCH IN CONTEXT

- 1. Systematic Review:** The authors performed a literature review encompassing pre-prints and published articles. They found that in sporadic Creutzfeldt-Jakob disease (sCJD), patient stratification based on the different histopathological subtypes is essential to prognosis and evaluating the efficacy of therapeutic treatments.
- 2. Interpretation:** The findings in this study highlight the spatio-temporal cascade of diffusion-weighted magnetic resonance imaging (DWI) abnormalities in seven molecular sCJD subtypes, confirming that each subtype presented a different cascade of lesion propagation. The proposed method provides an accurate, data-driven yet clinically reliable approach for *ante mortem* diagnosis of sCJD subtype. These features, together with the high inter-rater reliability, make the method suitable for implementation in clinical practice.
- 3. Future Directions:** The proposed method can be used for stratifying sCJD patients by molecular subtype in targeted clinical trials. Future studies should also consider using other biomarkers (e.g., Real-Time Quaking-Induced Conversion, RT-QuIC) together with DWI, with the aim to increase the accuracy of subtype diagnosis.

patients and the 50 controls, blind to the subtype diagnosis and the ratings of the other neuroradiologists. Of note, controls were included to perform the rating in an unbiased fashion, before the autopsy results became available. Thus the neuroradiologists were expecting positive and negative cases.

### 2.3 | Novel procedure for subtype diagnosis

#### 2.3.1 | Spatiotemporal cascades of DWI abnormalities

EBM<sup>19–21</sup> is a data-driven disease progression model that can estimate the temporal cascade of biomarker abnormality events in a disease from a *cross-sectional* dataset, that is, requiring patient data obtained at a single time point. Such estimation is feasible in a cohort of subjects encompassing a wide spectrum of disease severity because early biomarkers have a higher prevalence of abnormal values than the biomarkers that become abnormal later. In this work, 12 brain regional DWI hyperintensities were treated as biomarkers. We used DEBM<sup>23,24</sup> to estimate the spatiotemporal cascade of biomarker abnormality events for each sCJD subtype in a three-step process informed only by DWI ratings. First, DEBM estimates the degree of abnormality of each biomarker by linearly mapping the neuroradiologists' scores of each

subject to probabilities of regional abnormality (0: 0, 1: 0.33, 2: 0.67, 3: 1). Second, DEBM estimates the spatiotemporal cascade of events for each subject, by ordering these probabilities. Third, the mean spatiotemporal cascade for each subtype is estimated as the sequence that minimizes the sum of probabilistic Kendall's Tau distances to the spatiotemporal cascades of all subjects with the same sCJD subtype. Along with the mean cascades, the method also estimates a relative temporal distance between the biomarker abnormality events, resulting in a set of "event-centers" (EC) placed on a disease timeline normalized between 0 and 1.<sup>24</sup> To evaluate if the estimated cascades in the seven subtypes were significantly different from one another, we used permutation testing<sup>25</sup> as detailed in the Supplementary Material A.1.

The linear mapping to transform radiologists' scores into probabilities of regional abnormality is different from the usual approach in EBM, which is by mixture modeling<sup>19–21</sup>. In this work, we skipped the mixture modeling process as we observed a limitation in a recent article using the same dataset.<sup>19</sup> The EBM in that work<sup>19</sup> used a mixture of a Bernoulli distribution (modeling radiologists' scores 0 and 1) and a uniform distribution (modeling radiologists' scores 0 to 3), which mapped the two highest scores (2 and 3) to a likelihood of 1, thereby losing granularity in the degree of abnormality encoded in the ratings.

### 2.3.2 | Estimating the posterior probability for subtype diagnosis

Once the spatiotemporal cascades were estimated for all subtypes, we used them to estimate the probability that a test subject with his/her *PRNP129* genotype (MM / MV / VV) measured in vivo belongs to a particular subtype. We denote the spatiotemporal cascade of subtype *i* as  $S_i$ , and the spatiotemporal cascade of the test subject *j* estimated using the neuroradiologist's scores as  $s_j$ . The probability of subject *j* belonging to subtype *i* ( $P_{i,j}$ ) was calculated by measuring the atypicality of the test subject's cascade when compared to the spatiotemporal cascade of subtype *i*, using the probabilistic Kendall's Tau distance between the two cascades,  $d(s_j, S_i)$ :

$$P_{i,j} = \frac{p_{i,j} \times e^{-d(s_j, S_i)}}{\sum_i p_{i,j} \times e^{-d(s_j, S_i)}}$$

where  $p_{i,j}$  denotes the prevalence of the subtype *i* given the *PRNP129* genotype observed in subject *j*, in the general sCJD population. For example, for a subject with MV *PRNP129* genotype,  $p_{i,j}$  corresponding to subtypes MV1, MV2C, and MV2K were equal to their relative prevalence in the general sCJD population (Table S1), whereas the others were 0. The test subject *j* was assigned to the subtype with maximum  $P_{i,j}$ .

We also performed a supplementary analysis for subtype diagnosis without *PRNP129* genotype information. In this scenario, MM1 and its phenocopy MV1, as well as MM2 and its phenocopy MV2C, were considered in the same class. Thus  $p_{i,j}$  for these merged subtypes were obtained by adding their respective prevalence as specified in Table S1.

## 2.4 | Validation

We validated the proposed diagnostic method using 10-fold cross-validation, both with and without using *PRNP129* genotype information. We estimated the spatiotemporal cascades of the subtypes in the training set and used the subjects in the test set for calculating diagnostic accuracy. We calculated the individual sensitivity  $Sens_i$  for each sCJD subtype as the proportion of correctly identified patients (i.e., true positive  $TP_i$ ) over the total number  $N_i$  of patients with the subtype *i*:

$$Sens_i = TP_i / N_i$$

We computed balanced accuracy (BA) for each *PRNP129* genotype (MM, MV, VV) and overall. BA is defined as the average sensitivity of the subtypes under each *PRNP129* genotype and overall:

$$BA = \sum_i Sens_i / \sum_i 1$$

We also computed a weighted accuracy (WA) for each *PRNP129* genotype and overall, for measuring the expected diagnostic accuracy in clinical use considering the prevalence  $p_i$  of the subtypes in the general sCJD population (Table S1):

$$WA = \frac{\sum_i Sens_i \times p_i}{\sum_i p_i}$$

The obtained accuracies of the proposed model with *PRNP129* genotype information were benchmarked against those of the recently proposed decision tree classifier<sup>22</sup>. We used the same train-test splits in the 10-folds cross-validation for both methods. The decision tree algorithm was retrained and tested in each fold as detailed previously.<sup>22</sup> The significance of the difference between the accuracy of the two methods was assessed by using the studentized bootstrap<sup>26</sup> approach as detailed in the Supplementary Material A.2.

### 2.4.1 | Assessing rater dependency

We assessed the rater dependency of the proposed method by estimating the accuracies when using the same rater (rater 1) for training and testing (intra-rater accuracy) and by comparing them with the accuracies obtained when using different raters for testing (inter-rater accuracy). Details on this experiment are reported in the Supplementary Material A.3.

## 3 | RESULTS

### 3.1 | Patient's cohort

We included 488 sCJD subjects (median age at MRI, 65 years [interquartile range, 59–72]; 248 [51%] male) with positive MRI and

**TABLE 1** Demographics of sCJD patients according to subtype

Subtype	n (%)	Sex (M/F)	Age at MRI, years	Total disease duration, months	Time from onset to MRI, days	Time from MRI to death, days
MM1	216 (44.3)	114/102	66 (59-73)	2.6 (2.0-3.3)	47 (30-67)	28 (18-43)
MM2	43 (8.8)	20/23	66 (58-73)	12.7 (5.6-23.1)	91 (42-235)	242 (85-343)
MV1	40 (8.2)	22/18	67 (57-70)	4.1 (2.6-10.4)	69 (42-112)	39 (22-198)
MV2C	37 (7.6)	16/21	65 (61-69)	16.9 (9.8-24.2)	109 (54-285)	345 (156-547)
MV2K	36 (7.4)	20/16	64 (59-69)	12.2 (7.6-15.8)	158 (93-317)	112 (72-211)
VV1	25 (5.1)	13/12	56 (41-69)	9.7 (5.7-13.2)	120 (57-167)	168 (90-270)
VV2	91 (18.6)	43/48	65 (59-71)	5.0 (4.2-6.8)	99 (61-133)	61 (33-86)
Total	488 (100)	248/240	65 (59-72)	4.2 (2.5-8.8)	65 (37-126)	46 (23-111)

Median values with IQR are reported for time interval variables.

Abbreviations: IQR, interquartile range; MRI, magnetic resonance imaging; sCJD, sporadic Creutzfeldt-Jakob disease.

the following seven unmixed (pure) subtypes: MM1 ( $n = 216$ ), MM2 ( $n = 43$ ), MV1 ( $n = 40$ ), MV2C ( $n = 37$ ), MV2K ( $n = 36$ ), VV1 ( $n = 25$ ), VV2 ( $n = 91$ ). Demographic data of these patients are reported in Table 1 and the flowchart of patient selection is illustrated in Figure S1. Data from the subgroup of 150 sCJD patients selected for analyzing the rater dependency of the proposed method are reported in Table S2.

### 3.2 | Spatiotemporal propagation of DWI abnormalities is subtype specific

The proposed approach estimated the cascades for each of the seven subtypes. The results of permutation testing for all pairwise comparisons of the subtype cascades are shown in Table S3. The obtained cascades for the subtypes are described briefly in this section and have been elaborated further in supplementary material B. Representative DWI images of MM(MV)1, MM(MV)2C, VV1, MV2K, and VV2 subtypes at early and advanced stages of the spatiotemporal cascades are illustrated in Figure 1.

The two most frequent sCJD subtypes (MM1 and VV2) had opposite cascades (adjusted  $p$ -value < 0.0001) of lesion propagation (Figure 2). In MM1 subjects, the first region to be impacted (henceforth referred to as "epicenter") was the parietal cortex, with EC = 0.25, which slightly preceded the involvement of the precuneus (EC = 0.30). The caudate was impacted quite early in the sequence (EC = 0.51), while the impact on the hippocampus, cerebellum, and thalamus occurred at later stages (EC  $\geq$  0.90).

In VV2 subjects the caudate was the epicenter (EC = 0.21), followed by other central nuclei, the cingulate gyrus, and the cerebellum (EC range: 0.46 to 0.62). The frontal cortex became abnormal only at a late stage (EC = 0.85) and preceded the involvement of other neocortical regions.

The MM2 cascade significantly differed (adjusted  $p$ -value = 0.0175) from that of MM1, despite sharing the epicenter in the parietal cortex and the similarity of the cortical participation (Figure 3A). The major differences were the late participation of the striatum (especially the

caudate) in MM2 (EC = 0.92) along with the finding that all cortical regions were impacted before the subcortical ones.

The cascades of the two VV subtypes were almost reciprocally opposite (Figure 3C) (adjusted  $p$ -value < 0.0001). The VV1 cascade resembled that of MM1 (adjusted  $p$ -value = 0.30) with the same epicenter (the parietal cortex, EC = 0.25), but with the addition of an earlier lesion detected in the limbic structures (insula: EC = 0.27; cingulate: EC = 0.33). Notably, VV1 had the earliest involvement of the hippocampus among all subtypes.

Considering the MV subtypes, the MV1 cascade largely mimicked that of MM1 (adjusted  $p$ -value = 0.51); lesion propagation pathways were opposite in MV2C and MV2K (adjusted  $p$ -value < 0.0001) (Figure 3B). Essentially, MV2C shared the epicenter in the parietal cortex and the cascade with MM2 (adjusted  $p$ -value = 0.80), which was expected as the two subtypes are considered phenocopies. By contrast, MV2K showed a reversed cascade, with the epicenter in the striatum, and propagation mimicking that of VV2 (adjusted  $p$ -value = 0.35), except for a later impact on the cerebellum.

### 3.3 | Subtype diagnosis

Our diagnostic procedure with the inclusion of PRNP129 information obtained 76.5% balanced accuracy (i.e., an average of the subtype sensitivities) and 87.0% weighted accuracy (i.e., considering the prevalence of the subtypes in the general sCJD population) (Figure 4). Without PRNP129 information, these accuracies dropped to 48.9% and 73.2%, respectively (Figure S2).

For the two most common subtypes MM1 and VV2, our procedure with the PRNP129 information achieved individual sensitivities of 92.6% and 91.2%, respectively (Figure 4). The procedure also achieved 96% sensitivity for the rare VV1 subtype, where only one out of 25 VV1 patients was incorrectly diagnosed as VV2. However, about half of the times (53.5%) a true MM2 subject received the wrong diagnosis of MM1, while the reverse occurred rarely (7.4%). Among the MV heterozygote patients, good sensitivities were obtained for the MV2C

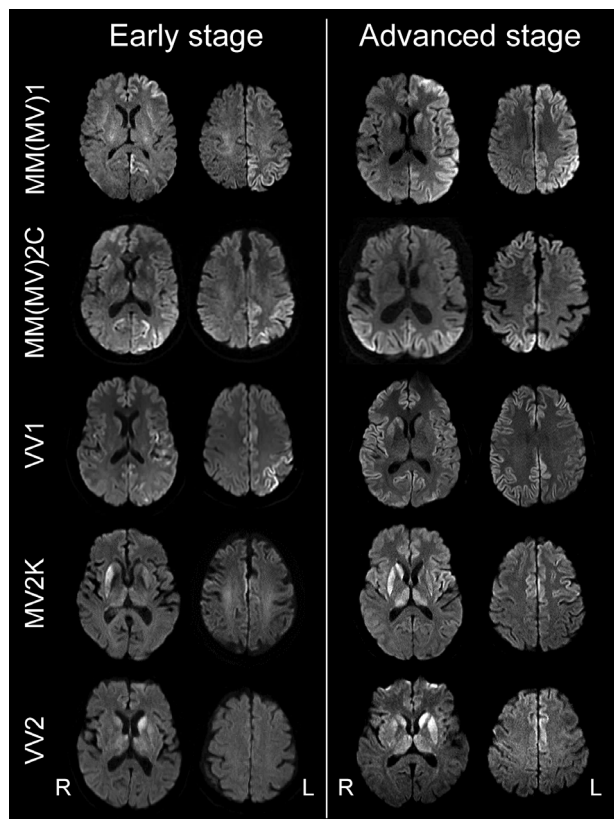


**FIGURE 1** Representative diffusion-weighted images of patients with different sCJD subtypes at early and advanced stage of disease. (First row) The early stage DWI of a patient with MM1 subtype who presented with hyperintensities in the left parietal cortex, including the precuneus, and in the anterior frontal cortical ribbon. The advanced stage DWI of a different MM1 patient showing asymmetric involvement of most of the cortex of the left cerebral hemisphere, in association with the caudate heads, the left cingulate, and the left insula. (Second row) The early stage DWI of a patient with MM2C subtype who presented with hyperintensities in the left parietal cortex including the precuneus. The advanced stage DWI of a different MV2C patient showing asymmetric involvement of the cortical ribbon; the striatum and thalami were spared. (Third row) The early stage DWI of a patient with VV1 subtype who presented with hyperintensities in the left parietal cortex, left cingulate and insula. The advanced stage DWI of a different VV1 patient showing extensive asymmetric involvement of the cerebral cortex and of the right striatum. The thalami and most of the left cerebral cortex were spared. (Fourth row) The early stage DWI of a patient with MV2K subtype who presented with asymmetric hyperintensities in the striatum and subtle bilateral hyperintensities in the posteromesial aspect of the thalami. The advanced stage DWI of a different MV2K patient showing asymmetric hyperintensities in the striatum and the whole thalami, along with mild involvement of the left frontal cortex and insula. The parietal cortex was spared. (Last row) The early stage DWI of a patient with VV2 subtype who presented with asymmetric DWI hyperintensities in the head of the caudate and in the anterior aspect of the putamen, along with very subtle hyperintensities in the thalami. The advanced stage DWI of a different patient with VV2 showing extensive hyperintensities in the striatum and thalami, as well as in the left cingulate and anterior frontal cortex. sCJD, sporadic Creutzfeldt-Jakob disease; DWI, diffusion-weighted imaging.

and MV2K subtypes (78.4% and 83.3%, respectively) and misdiagnosis between them was rare (only 1/37 [2.7%] and 4/36 [11.1%] cases, respectively). In contrast, MV1 was difficult to identify (sensitivity of 47.5%).

The comparative analyses of the current method with that based on the decision tree algorithm, when using *PRNP129* information, are shown in Table 2. The current method showed a significantly higher overall balanced accuracy than the decision tree (76.5% vs. 67.1%,  $p$ -value < 0.001), while the weighted accuracy was comparable (87.0% vs. 85.0%,  $p$ -value = 0.115). The accuracies were identical for the MM genotype (69.6% balanced and 89.8% weighted accuracy for both methods). Our method showed considerably higher balanced accuracy for the VV genotype than the decision tree (93.6% vs. 80.7%), while the weighted accuracies were similar (91.4% vs. 92.1%). Finally, in the MV genotype, the current method was more accurate than the decision tree (balanced accuracy: 69.7% vs. 56.5%; weighted accuracy: 70.6% vs. 57.3%).

The performances of the three neuroradiologists analyzing the same subset of 150 sCJD patients were similar as to the overall balanced accuracy (rater 1: 69% ± 11%; rater 2: 70% ± 10%, rater 3: 69% ± 9%) and the weighted accuracy (rater 1: 82% ± 5%; rater 2: 86% ± 5%, rater 3: 82% ± 5%) (Figure 5).

## 4 | DISCUSSION

We developed a diagnostic procedure supporting the *ante mortem* diagnosis of sCJD subtype in individual patients. The procedure cross-sectionally estimates the spatiotemporal cascades of the DWI signal hyperintensities in each subtype, in concert with the *PRNP129* genotype of the patients. We achieved 76.5% balanced accuracy among all subtypes, which raises to 87.0% if each subtype is weighted based on its prevalence in the general sCJD population. Without *PRNP129* genotype information in test subjects, the performance of the algorithm dropped to 73.2% weighted accuracy.

Unlike other popular machine learning algorithms, such as support vector machines or deep neural networks, the proposed method is not a *black box*, because the cascades of the DWI abnormalities can be meaningfully correlated to the clinical and histopathological features that distinguish each subtype. For instance, subtypes with opposite cascades, such as MV2C versus MV2K or VV1 versus VV2, were distinguished with high accuracy. This makes it easier to understand the decision process followed by the proposed diagnostic method and ensures its clinical usefulness.<sup>27,28</sup> For its implementation in clinical practice, the diagnostic procedure needs to work also with raters other than the one who trained the model. Our rater-dependency analysis showed that the accuracy of the proposed method is insensitive to the degree of the specific expertise of the neuroradiologists, making our method highly suitable for clinical practice. We also anticipate that the present approach is applicable to other neurodegenerative diseases, enhancing their differential diagnoses when MRI visual rating scores are acquired for the clinical evaluation of patients with suspected dementia.<sup>29</sup>

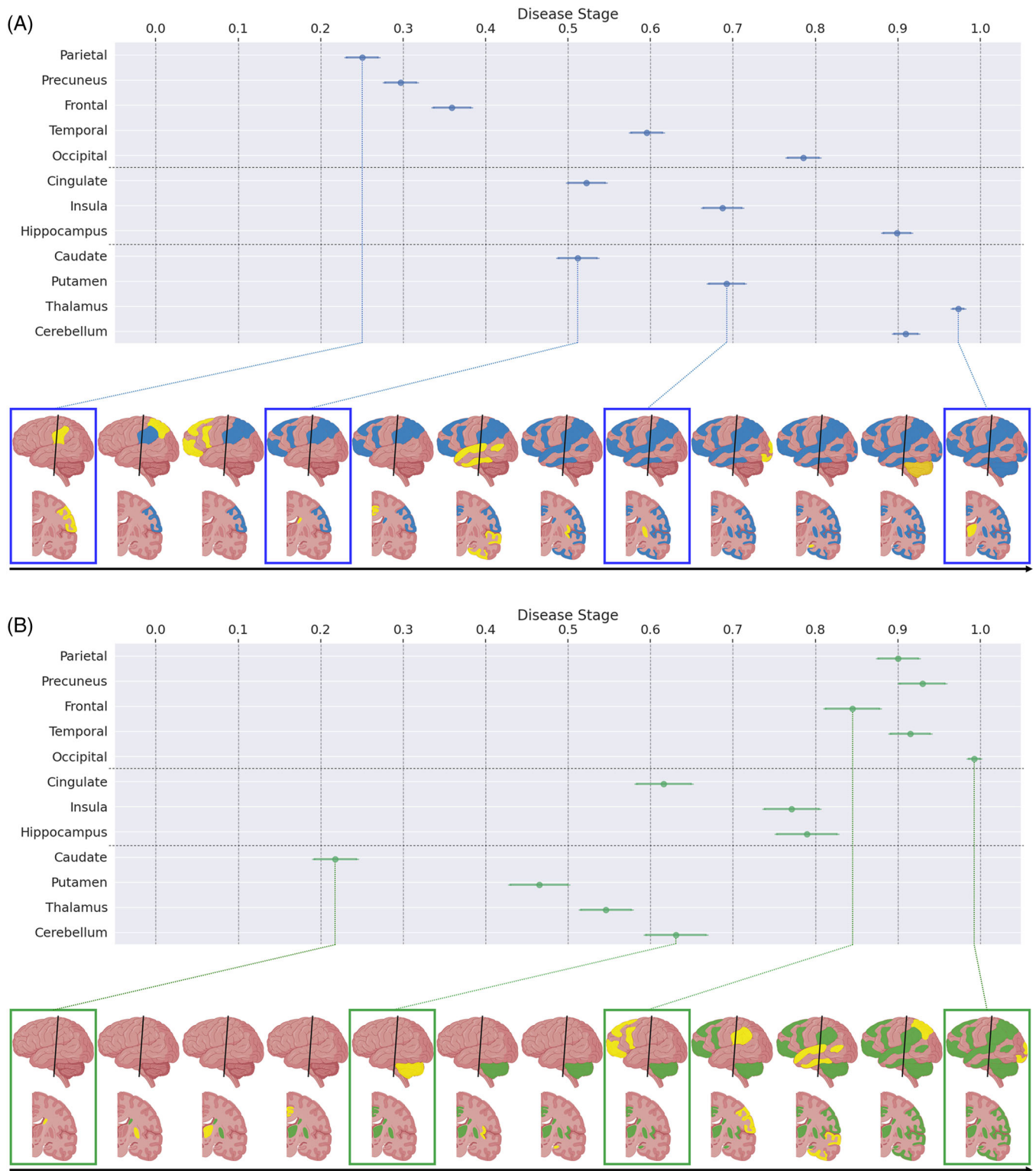


**FIGURE 2** Plot and pictorial representations of the spatiotemporal cascade as monitored by DWI in MM1 and VV2 subtypes. Plots and figures show the successive stages of the disease process as determined by the event centers in MM1 (A) and VV2 (B) subtypes. The times of the first detection of the impacted brain regions are indicated as points on a normalized interval between 0 and 1, along with their standard deviations represented by horizontal bars. Data are estimated from a set of 100 independent bootstrap samples. The figures visually highlight sagittal and coronal views of the brain regions that are impacted at the successive disease stages; yellow color identifies newly affected regions, blue (A) and green (B) colors identify previously affected regions. Created with BioRender.com. DWI, diffusion-weighted imaging

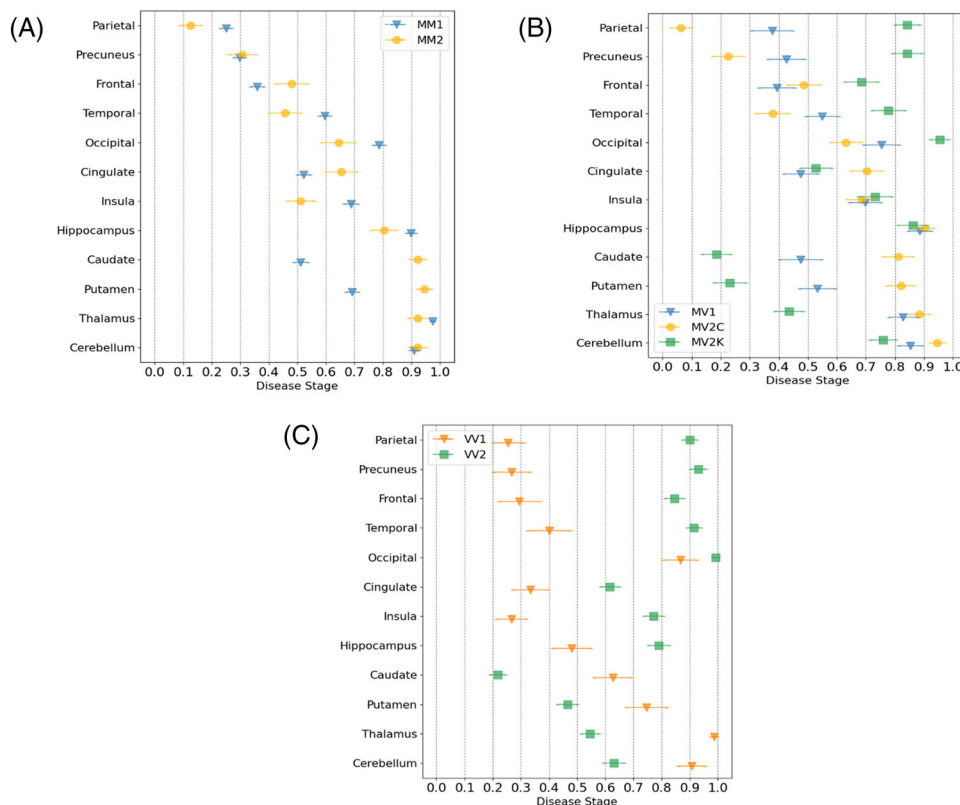


**FIGURE 3** Event-center plots comparing the spatiotemporal cascade of DWI abnormalities in sCJD subtypes grouped according to the *PRNP129* genotypes. Plots show the successive stages of the disease process as determined by the event centers for each sCJD subtype. The event center of each brain region is placed on a normalized disease stage timeline between 0 and 1 along with a horizontal error bar representing its standard deviation. Data were estimated from a batch of 100 independent bootstrap samples. (A) In the MM *PRNP129* genotype, patients with MM1 and MM2 shared the same epicenter in the parietal cortex, but then followed different orderings of propagation. The main difference was the caudate, affected early in MM1 and only very late in MM2. (B) In the MV *PRNP129* genotype, patients with MV1 and MV2C also shared the epicenter in the parietal cortex. The striatum was impacted quite early for MV1, while it was one of the last regions for MV2C. In contrast, the cascade of MV2K had epicenter in the striatum, followed by thalamus and cingulate; the frontal lobe was involved later and preceded the cortex of the other lobes in this subtype. (C) In the VV *PRNP129* genotype, VV1 cascade was opposite to that of VV2. The epicenter was located in the parietal cortex for VV1, while it was in the caudate for VV2. Disease propagation reached cortical and limbic regions very early in VV1; these regions were affected at the last stages in VV2, which instead was characterized by early involvement of the putamen, thalamus, and cerebellum. DWI, diffusion-weighted imaging; sCJD, sporadic Creutzfeldt-Jakob disease

**TABLE 2** Comparison between the diagnostic accuracy of the proposed method and a decision tree algorithm referred to each *PRNP129* genotype and to the entire cohort

Metric	MM		MV		VV		Total		p-value
	DEBM	Decision Tree	DEBM	Decision Tree	DEBM	Decision Tree	DEBM	Decision Tree	
Balanced accuracy	69.6	69.6	69.7	56.5	93.6	80.7	76.5	67.1	<0.001
Weighted accuracy	89.8	89.8	70.6	57.3	91.4	92.1	87.0	85.0	0.115

Balanced accuracy is defined as the average class sensitivity of the subtypes under each *PRNP129* genotype and overall. Weighted accuracy is the weighted average class sensitivity, where the weights are the subtype prevalences in the general sCJD population.

Abbreviations: DEBM, discriminative event-based model; sCJD, sporadic Creutzfeldt-Jakob disease.

Another recent study using a different EBM approach showed similar propagation cascades in the same patient cohort, further suggesting that the heterogeneity in the regional brain evolution of each type of disease is mostly due to the conformational characteristics of the asso-

ciated PrP<sup>D</sup> (i.e., prion strain).<sup>19</sup> Although overall the results of the two approaches were similar, some differences emerged. In particular, our novel approach indicated the caudate as the disease epicenter for VV2, whereas the cerebellum (overlapping with other subcortical regions)



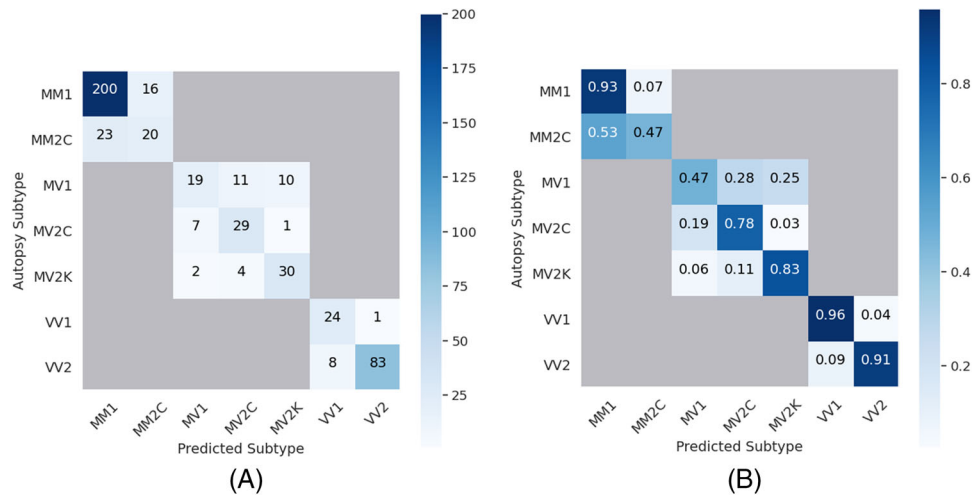


**FIGURE 4** Confusion matrix and normalized confusion matrix obtained with the proposed method using 10-fold cross-validation. The two matrices illustrate the diagnostic performance of the proposed method with *PRNP129* genotype information by comparing the subtype as classified at autopsy (rows) with the subtype diagnosed with the method (columns) for all patients in the test set, as determined with a 10-fold cross-validation scheme. The entries of the matrix are numbers of patients (A) and corresponding proportions (B). The diagonal elements in (A) represent the number of correctly diagnosed subjects and the off-diagonal elements represents the incorrectly diagnosed subjects. The diagonal elements in (B) represent the fraction of correctly diagnosed subjects in a specific subtype, while the off-diagonal elements represent the fraction of incorrectly diagnosed subjects. The overall balanced accuracy obtained was 76.5%, while the accuracy weighted for the subtype prevalence was 87.0%

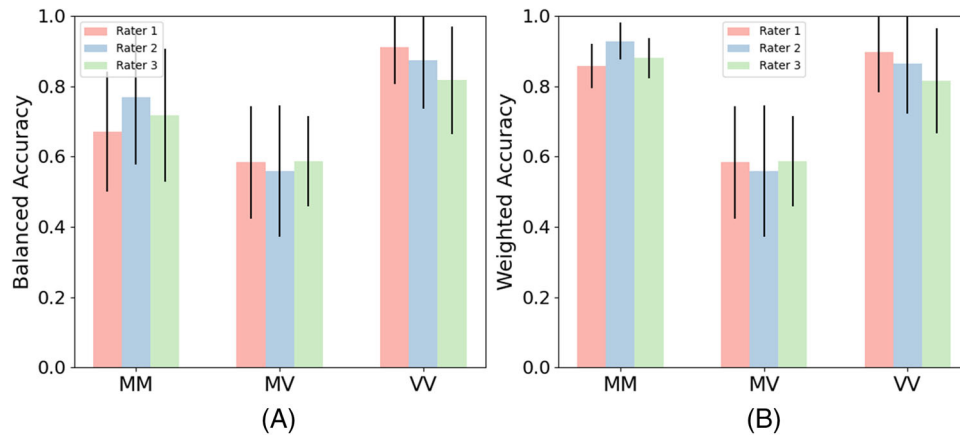


**FIGURE 5** Inter-rater performance analysis comparing balanced accuracies and weighted accuracies in the test set based on the scores of three neuroradiologists. Scores from rater 1 were used for training the model, while scores of the other two raters were only used in the test set. The height of the color-coded bar represents the balanced (A) and weighted (B) accuracy for each specific *PRNP129* genotype referred to each rater; the error bar indicates the standard deviation of the measurement computed in 30 iterations of randomized train-test split.

was the most probable epicenter according to EBM. The epicenter in the cerebellum would be more compatible with the usual clinical presentation of patients with VV2 characterized by an early onset of cerebellar symptoms and signs.<sup>8,30</sup> However, the lower sensitivity of DWI to alteration in the cerebellum, even when cerebellar involvement is clinically and neuropathologically unambiguous<sup>31</sup>, may explain the earlier impact on the caudate in DEBM. DWI alterations in the striatum are a well-known hallmark of sCJD,<sup>13,22</sup> and they are probably a more reliable biomarker for early diagnosis of VV2, as when determined by DEBM.

The ability to compute approximate estimates of the cascade in each individual is a unique feature of DEBM, which enabled the development of this novel diagnostic procedure through the comparative analysis of the individual estimate with each subtype-specific cascade and, with that, the identification of the most probable sCJD subtype. DEBM benefited also from the relatively large number of rarer subtypes (e.g., MV2C and VV1) in our cohort, which was a strength of this study and necessary to reconstruct the spatiotemporal cascades for all subtypes and to develop a reliable diagnostic procedure on a more balanced dataset among the subtypes.

The proposed method and the previously utilized decision tree algorithm<sup>22</sup> achieved high overall accuracies applying the same cross-validation scheme. Statistically, these results are consistent with those previously reported under a different cross-validation scheme, that is, with a held-out test set (88.6% weighted accuracy, [83.1% - 92.8%] 95% confidence interval).<sup>22</sup> Combined, these observations suggest that both methods can generate accurate and clinically useful results. Remarkably, the two methods performed similarly for the most common subtypes (MM1 and VV2), which combined account for almost 80% of the sCJD cases<sup>8,10</sup>. DEBM, however, could be particularly useful to identify the rarer subtypes<sup>8,10</sup> including MV2C, MV2K, and VV1 for which it reached higher sensitivities. This improved accuracy of the DEBM classifier, especially within the MV group, stems from the use of the cascades of all subtypes, including the rarer ones. On the contrary, the previous decision tree algorithm was not developed to account for this crucial information: it was able to discover multiple lesion distribution patterns associated with different phases of the disease for the most common subtypes, but only one pattern for each of the rarer subtypes.

One limitation of this study is that the entire procedure is based on the scores assigned to the DWI abnormalities in 12 brain regions by neuroradiologists. Although DWI has emerged as a very sensitive diagnostic modality and probably the test of choice for the diagnosis of sCJD at onset,<sup>13-18</sup> the expertise of the radiologist remains a major factor influencing the correct diagnosis. In particular, we estimated that radiologists can miss the diagnosis of sCJD in 5% to 10% of patients<sup>13</sup> and subtype diagnosis cannot be performed in this small percentage of cases, since our procedure is based only on positive MRI studies. Future work should focus on developing automated methods for estimating the severity of DWI signal abnormalities in the entire brain and for increasing DWI sensitivity. Another limitation of DEBM is the assumption that each subtype has a unique spatiotemporal cascade of DWI abnormalities, which implies that some intra-subtype heterogeneity may not be captured by our model, limiting its diagnostic performance. Therefore, developing a model that could take into account such heterogeneity would likely increase the diagnostic accuracy obtainable with DWI. We have to acknowledge also that our model has been developed only for the "pure" sCJD subtypes and therefore it cannot be used to recognize mixed sCJD subtypes in which, at this time, only the dominant subtype may be diagnosed. A final limitation was that, despite an evident imbalance in the timing of MRI concerning the course of the disease in the different subtypes, our model was intended to estimate only the sequence of progression, and not the rate of progression. Since the prediction of subtype is based on a single timepoint DWI, we were unable to calculate or use the rate of progression in the modelling, which is an information that future works should consider to include.

Regarding other clinical implications of the proposed method, the MRI finding that a specific and focal region of the brain or epicenter is initially impacted can help the radiologist to raise the suspicion of prion disease at an earlier stage. Furthermore, knowledge of the spatiotemporal cascades of DWI abnormalities may help to corroborate the initial findings by monitoring and comparing follow-up MRI examinations increasing the prognostic accuracy. The subtype diagnosis of

sCJD patients is also essential for optimizing the design of future clinical trials, because it allows the identification of more homogeneous groups of patients at disease onset, thus potentially influencing the selection of the most appropriate treatment and increasing the time window for therapeutic intervention.<sup>32</sup>

In 2008, a highly sensitive approach to the diagnostic detection of PrP<sup>D</sup> in the cerebrospinal fluid from patients suspected of having a prion disease was introduced under the name of real-time quaking-induced conversion (RT-QuIC).<sup>33</sup> RT-QuIC is based on the propensity of PrP<sup>D</sup>, even when present in minute amounts, to act as an *in vitro* seed to convert PrP<sup>C</sup>, offered as substrate, to PrP<sup>D</sup> until it becomes detectable. Foutz and coworkers, leveraging an advanced version of RT-QuIC, suggested that differences in lag time and amplitude of seeding activity can distinguish between major sCJD subtypes, especially when the *PRNP129* polymorphism is known.<sup>34</sup> A future approach coupling DWI event-based modeling and RT-QuIC, may further increase the *ante mortem* diagnostic accuracy of sCJD subtypes.

In conclusion, we proposed a novel and explainable diagnostic procedure for identifying the sCJD subtype in individual patients. The procedure relies on the distinct spatiotemporal cascade of lesions detected with diffusion MRI. We achieved state-of-the-art performance in identifying sCJD subtype *ante mortem*, and the proposed method could aid early disease prognosis and the accurate identification of patient cohorts for clinical trials.

#### ACKNOWLEDGMENTS

V.V., R.P., S.K., and A.B. have received funding from the European Union's Horizon 2020 research and innovation programme under grant agreement No. 666992. A.B. has received funding from the CJD Foundation (CJD Foundation Grant, Strides for CJD Grant, Walter Williams Memorial Research Grant, Sherry Maxwell Fabian Memorial Grant, Jeffrey A. Smith Memorial Research Grant). M.L.C. and B.S.A. are supported by CDC NU2GCK000434. This work was partially supported by the Italian Ministry of Health (RRC). The funding sources had no involvement in study design, in the collection, analysis, and interpretation of data, in the writing of the report, nor in the decision to submit the article for publication.

The findings and conclusions in this report are those of the authors and do not necessarily represent the official position of the Centers for Disease Control and Prevention, Atlanta, Georgia, USA.

Open access funding provided by BIBLIOSAN.

#### CONFLICT OF INTEREST

B.S. Appleby: Has received research funding from CDC, NIH, Ionis, and Alector. Consulting for Acadia, Ionis, and Sangamo. Received royalties from Wolters Kluwer. Received payment for expert testimony for Kaufman & Canoles. Received support for meetings/travel from the CJD Foundation. Holds unpaid leadership roles for the Alzheimer's Association and CJD Foundation.

V. Venkatraghavan, R. Pascuzzo, E.E. Bron, M. Moscatelli, M. Grisoli, A. Pickens, M.L. Cohen, L.B. Schonberger, P. Gambetti, S. Klein, A. Bizzi: Nothing to disclose.

Author disclosures are available in the [Supporting Information](#).

## ORCID

Riccardo Pascuzzo  <https://orcid.org/0000-0001-6555-1784>

## REFERENCES

- Prusiner SB. Cell biology. A unifying role for prions in neurodegenerative diseases. *Science*. 2012;336:1511-1513.
- Gambetti P, Cali I, Notari S, Kong Q, Zou WQ, Surewicz WK. Molecular biology and pathology of prion strains in sporadic human prion diseases. *Acta Neuropathol*. 2011;121:79-90.
- Puoti G, Bizzi A, Forloni G, Safar JG, Tagliavini F, Gambetti P. Sporadic human prion diseases: molecular insights and diagnosis. *Lancet Neurol*. 2012;11:618-628.
- Parchi P, Giese A, Capellari S, et al. Classification of sporadic Creutzfeldt-Jakob disease based on molecular and phenotypic analysis of 300 subjects. *Ann Neurol*. 1999;46:224-233.
- Gambetti P, Kong Q, Zou W, Parchi P, Chen SG. Sporadic and familial CJD: classification and characterisation. *British Medical Bulletin*. 2003;66:213-239.
- Parchi P, Strammiello R, Notari S, et al. Incidence and spectrum of sporadic Creutzfeldt-Jakob disease variants with mixed phenotype and co-occurrence of PrPSc types: an updated classification. *Acta Neuropathol*. 2009;118:659-671.
- Parchi P, De Boni L, Saverioni D, et al. Consensus classification of human prion disease histotypes allows reliable identification of molecular subtypes: an inter-rater study among surveillance centres in Europe and USA. *Acta Neuropathol*. 2012;124:517-529.
- Zerr I, Parchi P. Sporadic Creutzfeldt-Jakob disease. In: Pocchiari M, Manson J, eds. *Handbook of Clinical Neurology*. Elsevier; 2018:155-174.
- Nemani SK, Xiao X, Cali I, et al. A novel mechanism of phenotypic heterogeneity in Creutzfeldt-Jakob disease. *Acta Neuropathol Commun*. 2020;8:85.
- Collins SJ, Sanchez-Juan P, Masters CL, et al. Determinants of diagnostic investigation sensitivities across the clinical spectrum of sporadic Creutzfeldt-Jakob disease. *Brain*. 2006;129:2278-2287.
- Mead S, Burnell M, Lowe J, et al. Clinical trial simulations based on genetic stratification and the natural history of a functional outcome measure in Creutzfeldt-Jakob disease. *JAMA Neurol*. 2016;73:447-455.
- Teruya K, Doh-Ura K. Insights from therapeutic studies for PrP prion disease. *Cold Spring Harb Perspect Med*. 2017;7:a024430.
- Bizzi A, Pascuzzo R, Blevins J, et al. Evaluation of a new criterion for detecting prion disease with diffusion magnetic resonance imaging. *JAMA Neurol*. 2020;77:1141-1149.
- Young G, Geschwind M, Fischbein N, et al. Diffusion-weighted and fluid-attenuated inversion recovery imaging in Creutzfeldt-Jakob disease: high sensitivity and specificity for diagnosis. *Am J Neuroradiol*. 2005;26:1551-1562.
- Tschampa H, Kallenberg K, Urbach H, et al. MRI in the diagnosis of sporadic Creutzfeldt-Jakob disease: a study on inter-observer agreement. *Brain*. 2005;128:2026-2033.
- Meissner B, Kallenberg K, Sanchez-Juan P, et al. MRI lesion profiles in sporadic Creutzfeldt-Jakob disease. *Neurology*. 2009;72:1994-2001.
- Vitali P, Maccagnano E, Caverzasi E, et al. Diffusion-weighted MRI hyperintensity patterns differentiate CJD from other rapid dementias. *Neurology*. 2011;76:1711-1719.
- Bizzi A, Peoc'h K. Amended diagnostic protocol increases the early diagnosis of sporadic Creutzfeldt-Jakob disease. *Neurology*. 2018;91:155-156.
- Pascuzzo R, Oxtoby NP, Young AL, et al. Prion propagation estimated from brain diffusion MRI is subtype dependent in sporadic Creutzfeldt-Jakob disease. *Acta Neuropathol*. 2020;140:169-181.
- Fonteijn HM, Modat M, Clarkson MJ, et al. An event-based model for disease progression and its application in familial Alzheimer's disease and Huntington's disease. *Neuroimage*. 2012;60:1880-1889.
- Young AL, Oxtoby NP, Daga P, et al. A data-driven model of biomarker changes in sporadic Alzheimer's disease. *Brain*. 2014;137:2564-2577.
- Bizzi A, Pascuzzo R, Blevins J, et al. Subtype diagnosis of sporadic Creutzfeldt-Jakob disease with diffusion magnetic resonance imaging. *Ann Neurol*. 2021;89:560-572.
- Venkatraghavan V, Bron EE, Niessen WJ, Klein S. A discriminative event based model for Alzheimer's disease progression modeling. In: Niethammer M, Styner M, Aylward S, eds. *Information Processing in Medical Imaging. IPMI 2017. Lecture Notes in Computer Science*. Springer; 2017:121-133.
- Venkatraghavan V, Bron EE, Niessen WJ, Klein S. Alzheimer's Disease Neuroimaging Initiative. Disease progression timeline estimation for Alzheimer's disease using discriminative event based modeling. *Neuroimage*. 2019;186:518-532.
- Wilcox RR. *Applying contemporary statistical techniques*. Elsevier; 2003.
- Davison AC, Hinkley DV. *Bootstrap methods and their application*. Cambridge University Press; 1997.
- Cabitzza F, Rasoini R, Gensini GF. Unintended consequences of machine learning in medicine. *JAMA*. 2017;318:517-518.
- Rajkomar A, Dean J, Kohane I. Machine learning in medicine. *N Engl J Med*. 2019;380:1347-1358.
- Harper L, Fumagalli GG, Barkhof F, et al. MRI visual rating scales in the diagnosis of dementia: evaluation in 184 post-mortem confirmed cases. *Brain*. 2016;139:1211-1225.
- Baiardi S, Magherini A, Capellari S, et al. Towards an early clinical diagnosis of sporadic CJD VV2 (ataxic type). *J Neurol Neurosurg Psychiatry*. 2017;88:764-772.
- Cohen OS, Hoffmann C, Lee H, Chapman J, Fulbright RK, Prohovnik I. MRI detection of the cerebellar syndrome in Creutzfeldt-Jakob disease. *Cerebellum*. 2009;8:373-381.
- Forloni G, Roiter I, Tagliavini F. Clinical trials of prion disease therapeutics. *Curr Opin Pharmacol*. 2019;44:53-60.
- Atarashi R, Wilham JM, Christensen L, et al. Simplified ultrasensitive prion detection by recombinant PrP conversion with shaking. *Nat Methods*. 2008;5:211-212.
- Foutz A, Appleby BS, Hamlin C, et al. Diagnostic and prognostic value of human prion detection in cerebrospinal fluid. *Ann Neurol*. 2017;81:79-92.

## SUPPORTING INFORMATION

Additional supporting information can be found online in the Supporting Information section at the end of this article.

**How to cite this article:** Venkatraghavan V, Pascuzzo R, Bron EE, et al. A discriminative event-based model for subtype diagnosis of sporadic Creutzfeldt-Jakob disease using brain MRI. *Alzheimer's Dement*. 2023;1-11.  
<https://doi.org/10.1002/alz.12939>